Rough Surface Analysis using Kirchhoff Theory

Hossein Ragheb * and Edwin R. Hancock
Department of Computer Science
University of York, York, YO1 5DD, UK.
hossein,erh@cs.york.ac.uk

Abstract

In this paper we illustrate the use of the Beckmann-Kirchhoff model for analysing rough surface reflectance. The Beckmann-Kirchhoff model is a physical model that describes the reflectance of light from rough surfaces. The parameter of the model is the surface slope, or ratio of the surface roughness to the correlation length. We show how this parameter may be estimated using pairs of surface images, subject to different illumination directions. With the parameter to hand, the Beckmann-Kirchhoff model may be used to perform Lambertian reflectance correction, and hence shape-from-shading may be applied to the rough surfaces. The model may also be used for surface re-illumination. We present experiments to illustrate the utility of the method for each of these tasks.

1 Introduction

Reflectance modelling is a task of pivotal importance in the analysis of image data by computer. For instance, in computer graphics it is necessary for generating realistic images of synthetic scenes. In computer vision, on the other hand, reflectance models form the basis of surface analysis techniques such as shape-from-shading and photometric stereo, and may also be used to estimate the physical properties of materials from passively sensed image data [5]. The simplest and most commonly used model is Lambert's law which can be used to describe diffuse reflectance from matte surfaces of constant albedo. However, although convenient due to the fact that the observed brightness is independent of viewer direction, Lambert's law fails to accurately describe reflectance from both rough and shiny surfaces. Hence, there has been considerable recent effort to developing more complex models of the reflectance process. Hence, Wolff [12] has used the Fresnel term to model refractive attenuation in shiny surfaces, while Oren and Nayar [12] have a semi-empirical model that can be used to model departures from Lambert's law for rough surfaces.

Despite these advances, the analysis of rough surfaces still poses an important challenge. Roughness is a measure of the statistical variation in the topographic relief of a surface [3]. Hence, the reflectance from rough surfaces represents an important class of texture. There are many ways in which roughness can be characterised. However, in physics it is the surface roughness, σ, and the correlation length, T, that are most commonly used to represent the height distribution and the spatial scale of surface roughness. The height distribution is frequently assumed to be Gaussian [8], while the correlation length has been modelled using both Gaussian [2] and exponential [8] distributions. Although the exponential distribution gives a better fit to the data, since the derivative is discontinuous at the origin, it can lead to problems in estimating higher order surface

*Sponsored by the university of Bu-Ali Sina, Hamedan, Iran.

properties, such as surface gradients. Another way of characterising roughness is to use the RMS slope, i.e. the ratio of the RMS roughness to the correlation length [4]. However, reliable estimation of the RMS slope has proved to be an elusive problem [3].

In this paper we are interested in using reflectance models to analyse the surface properties and shape of rough surfaces. The effect of variable surface roughness is to alter the relative contributions of the specular and diffuse reflectance to the total reflectance. The Torrance-Sparrow model [10] is among the most popular models which aims to incorporate the effect of roughness into the specular reflectance component. The calculation of reflectance is based on geometrical optics, and is hence applicable when the surface irregularities are much larger than the wavelength of incident radiation. Nayar et al. [7] showed that under these conditions the Torrance-Sparrow model approximates the physical optics model developed by Beckmann and Spizzichino [2]. Alternative physical-optics approaches to the problem of specular reflection from rough surfaces can be found in the literature [1, 6, 12]. One of the shortcomings of these aforementioned models is that they ignore the effect of roughness on the diffuse reflectance component. However, this effect has been incorporated into the model developed by Oren and Nayar [12]. The major drawback of both the Torrance-Sparrow model and the Oren-Nayar model is that they rely on the assumption of surface isotropy and this in turn requires that the cavities associated with roughness have no preferred direction. Obviously, such isotropic cavitated surfaces cannot exist, because they are inconsistent with surface geometry [5]. Based on this observation, Ginneken et al. have recently developed a model that can be used to predict reflectance from isotropic rough surfaces that have both specular and diffuse components [5]. The parameters of their model are the surface roughness measured in terms of the RMS slope, the albedo, and the balance between the diffuse and specular components. They also claim that the model can be used to predict changes in surface texture as the illumination and viewing angles vary.

However, the scalar theory of scattering from rough surfaces developed by Beckmann [2] may offer and interesting alternative to these computational models. The Beckmann model commences from the Helmholtz-Kirchhoff diffraction integral [8]. To overcome some problems involved in solving this integral, an approximation known as the Kirchhoff boundary condition is made. This approximation limits the validity of the scalar theory to the case of scattering close to the specular direction. However, it should be noted that the polarization properties of the scattered light are not accounted for by this model. Beckmann has used the Kirchhoff scatter theory to develop reflectance models that can be applied to surfaces with different scales of roughness, i.e. slightly-rough, moderately-rough and very-rough surfaces. These models also give different scattering behaviour when the form of the surface correlation function is varied. For very-rough surfaces, Beckmann has explored the effects of Gaussian and exponential correlation functions. In its original form, this model is limited to the case of scattering close to the specular direction. However, Vernold and Harvey [11] have recently modified the Beckmann model to overcome this limitation and have extended the model to large angles of both incidence and scatter.

One of the problems with Beckmann-Kirchhoff theory is that it is not at first sight particularly well suited for use in computer vision because of its mathematical structure. The aim in this paper is to explore whether the model can be used to analyse rough surfaces. We commence by showing how the model can be used to estimate the surface slope parameter. With this parameter to hand the model may be used to recover corrected Lambertian reflectance, and hence standard shape-from-shading methods may be applied to

rough surfaces. The recovered surface may be re-illuminated using the rough reflectance predictions of the Beckmann model.

2 Beckmann-Kirchhoff Scatter Theory

In this paper, we confine our attention to the exponential correlation function since it gives a better fit to measured surface data for very-rough surfaces [3, 8]. Under this restriction, the diffuse reflectance function which results from Beckmann's model is

$$I(\theta_i, \theta_r, \phi_r) \approx 2\pi F^2(\theta_i, \theta_r, \phi_r) T^2 / A v_z^2 \sigma^2 (1 + v_{xy}^2 T^2 / v_z^2 \sigma^2)^{3/2} \quad (1)$$

The geometrical factor $F(\theta_i, \theta_r, \phi_r)$ is given by

$$F(\theta_i, \theta_r, \phi_r) = (1 + \cos\theta_i \cos\theta_r - \sin\theta_i \sin\theta_r \cos\phi_r) / \cos\theta_i (\cos\theta_i + \cos\theta_r)$$

The model depends on both the incidence and the reflectance angles. In the above equation θ_i and ($\phi_i = \pi$) are the zenith and azimuth angles of the illuminant and θ_r and ϕ_r are the zenith and azimuth angles of the viewer (on local tangent planes). Also, $v_x = k(\sin\theta_i - \sin\theta_r \cos\phi_r)$, $v_y = -k(\sin\theta_r \sin\phi_r)$, $v_z = -k(\cos\theta_i + \cos\theta_r)$, $v_{xy}^2 = v_x^2 + v_y^2$ and $k = 2\pi/\lambda$, where λ is the wavelength. The physical properties of the surface are captured by the surface slope $m = \sigma/T$ which is given in terms of the surface roughness σ and the correlation length T. This equation may also be used to model the total reflectance since the specular contribution is negligible for very-rough surfaces. The parameter A is the area of a plane sheet on which the scattering coefficient is defined [2]. This parameter is only effective when computing the absolute scattered intensity. However, since it originally comes from the instrumentation characteristics, we do not consider it as a physical surface property. In Section 3, after estimating surface slope, we also describe how an approximate value for A can be found.

2.1 Modification of Vernold-Harvey

The Beckmann model fails for large incidence angles and large scattering angles. To overcome this problem, Vernold and Harvey [11] have recently developed a modification of the Beckmann model that gives excellent agreement with experimental scattering data from rough surfaces at both large angles of incidence and at large scatter angles. The failure of the Kirchhoff theory to handle wide-angle scattering and large angles of incidence has been highlighted by other authors [4] too. Although Vernold and Harvey [11] agree with the observation that the local and mean surface normals do not coincide, they do not agree that a new obliqueness factor must be derived using the local surface normal. Instead, they claim that it is appropriate to use the mean surface normal when modelling rough surfaces, under conditions where the scale of the test or probe beam is much larger than the spatial scales under study. In the Vernold and Harvey modification [11], the geometrical factor (F^2) used in the Beckmann model is replaced by the cosine of the incidence angle which comes from Lambert's cosine reflectance law. They have applied their modification to that variant of the Beckmann model which assumes a Gaussian correlation function for the surface. Here, we apply their modification to the Beckmann model for very-rough surfaces with an exponential correlation function. Hence, by replacing the term F^2 with $\cos\theta_i$ in Eq. (1), the reflectance function for the modified B-K model is

$$I(\theta_i, \theta_r, \phi_r) = 2\pi \cos(\theta_i) / A v_z^2 m^2 [1 + v_{xy}^2 / (v_z^2 m^2)]^{3/2} \quad (2)$$

3 Surface Slope Estimation

For very-rough dielectric surfaces, we can use the B-K model to estimate the surface slope $m = \sigma/T$. Note that the quantity $\sigma\sqrt{2}/T$ has also been referred to as the RMS gradient

σ_g [8]. Furthermore, Caron et al. [4] have recently computed the angle of RMS slope given by $\theta_0 = \pi/2 - \tan^{-1}(\sqrt{2}m)$. They have shown that for incidence angles smaller than θ_0, the reflectance predictions delivered by the Kirchhoff theory are reliable. Once an estimate of m is to hand, we can fit the B-K diffuse reflectance model to the data. Such a model is potentially useful since it allows photometric correction to be performed and the Lambertian reflectance component to be recovered.

Our technique for estimating the surface slope $m = \sigma/T$ is as follows. First, we collect images with two different angles of illumination. Using the two images we make measurements of the reflectance I_1, I_2 at a corresponding point on the surface. This is straightforward in practice since we keep the surface fixed and move the light-source direction. Let the two different angles of incidence be $\theta_i = \theta_1$ and $\theta_i = \theta_2$. In both images the planar surface is perpendicular to the viewing direction, i.e. $\theta_r = 0$. To deal with problems of local texture arising from the surface roughness, we average the intensities over local neighborhoods. Although the use of two different wavelengths is possible, here we use only one wavelength λ. Under these illumination conditions and from Section 2 we can write $v_{xy}(\theta_i) = (2\pi/\lambda)\sin(\theta_i)$ and $v_z(\theta_i) = (2\pi/\lambda)[1+\cos(\theta_i)]$. We use the average quantities to compute the ratio I_1/I_2. From Eq. (2) the intensity ratio is given by

$$\frac{I_1}{I_2} = \frac{\cos(\theta_1)v_z^2(\theta_2)}{\cos(\theta_2)v_z^2(\theta_1)} \left\{ \frac{1+v_{xy}^2(\theta_2)/[v_z^2(\theta_2)m^2]}{1+v_{xy}^2(\theta_1)/[v_z^2(\theta_1)m^2]} \right\}^{3/2} \tag{3}$$

Hence, the estimate of surface slope parameter $m = \sigma/T$ is given by

$$m = \left\{ \frac{1}{K-1} \left[\frac{v_{xy}^2(\theta_2)}{v_z^2(\theta_2)} - K\frac{v_{xy}^2(\theta_1)}{v_z^2(\theta_1)} \right] \right\}^{1/2} \tag{4}$$

where $K = \{[\cos(\theta_2)v_z^2(\theta_1)I_1]/[\cos(\theta_1)v_z^2(\theta_2)I_2]\}^{2/3}$. By substituting one of the two pairs (I_1, θ_1) or (I_2, θ_2) together with λ and m into Eq. (2), an estimate of the parameter A can also be obtained. The absolute scattered intensity for any illumination condition can be computed using Eq. (2) together with the estimates of m and A.

4 Photometric Correction for SFS

With estimates of the surface slope parameter $m = \sigma/T$, we may use the diffuse reflectance model of Eq. (2) to perform surface analysis. We commence by considering how the model may be used to perform photometric correction and hence recover the Lambertian reflectance component $I_L = \cos(\theta_i)$ from the raw diffuse reflectance. With corrected Lambertian reflectance to hand, we can apply conventional shape-from-shading techniques to recover shape (surface normal) information. Recently, we have proposed the photometric correction approach for semi-empirical reflectance models in [9].

4.1 Model As a Function of Incidence Angle

For some problems in computer vision, such as shape-from-shading, it is the incidence angle behavior of the reflectance models that is of primary interest. Hence, here we derive a formulation for the specific case when the angle between the light-source and the viewing directions is small, and so $\theta_i = \theta_r$ and $\phi_r = \pi$. In shape-from-shading only one image of the object is available. When the light source and viewing directions are identical, the maximum fraction of the surface is illuminated and visible. Under these

conditions the reflectance equation can be simplified by replacing the quantities $v_{xy} = v_x = 2k\sin(\theta_i)$ and $v_z = -2k\cos(\theta_i)$ in Eq. (2). Hence, the modified B-K model for this case is

$$I(\theta_i) \approx \lambda^2/8\pi A m^2 \cos(\theta_i)[1+(\tan^2(\theta_i)/m^2)]^{3/2} \quad (5)$$

In Fig. 1, we show the behaviour of the modified B-K model. The different curves in each panel show the diffuse intensity I as a function of the incidence angle θ_i for different values of surface slope $m = \sigma/T$. The dashed curve in each panel is the prediction of Lambert's cosine law. The plots are for a wavelength of $700nm$. The left panel (a) is for the case where the light-source and the viewing directions are identical, i.e. $\theta_i = \theta_r$ and $\phi_r = \pi$, while there is no restriction for the surface shape (Eq. 5). From the different curves it is clear that the larger the surface slope, (i.e. the surface roughness σ with respect to the correlation length T), the higher the diffuse intensity. In particular, for $m = 1.6$ and $m = 1.8$, the brightening effects are very intense compared to the Lambertian reflectance curve. In the right panel (b), the light-source direction is perpendicular to the viewing direction while the surface is assumed to be parabolic (i.e. one of zero Gaussian curvature) with the minimum (zero) curvature direction along the y axis. Hence $\theta_i = \pi/2 - \theta_r$ and $\phi_r = 0$. The equation for this specific case can be derived from Eq. (2). Here, by contrast with the top panel, as the surface slope decreases from $m = 1.8$ to $m = 1.0$, then so the diffuse intensity increases. Also, the maximum intensity moves away from $\theta_i = 0$ and occurs when the incidence angle is close to $\theta_i = 25^\circ$. This behaviour also means that the reflectance function is not injective, and so, not invertible.

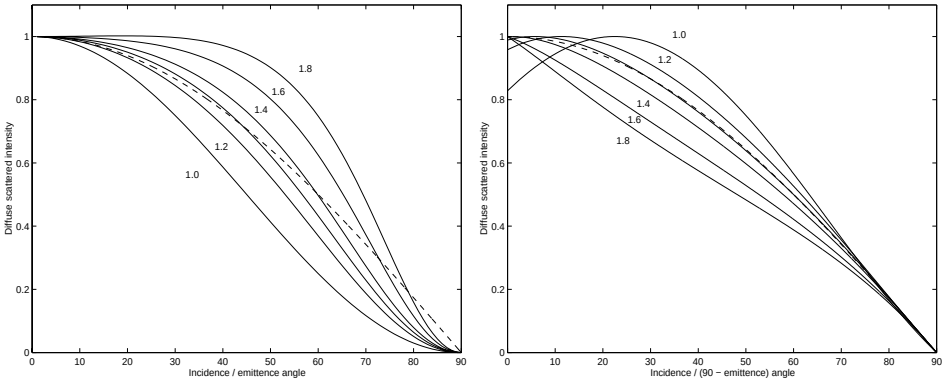

Figure 1: Diffuse intensity by the modified B-K model vs incidence angle (degrees) for surface slopes $m = 1.0, 1.2, .., 1.8$ compared to Lambertian model (dashed) for two illumination conditions: (a) $\theta_i = \theta_r$ and $\phi_r = \pi$ (left), (b) $\theta_i = \pi/2 - \theta_r$ and $\phi_r = 0$ on surfaces with parabolic shapes (right).

4.2 Lookup Table Solution

We can not recover the Lambertian reflectance component $\cos(\theta_i)$ directly from the modified B-K model since the analytic solution of the resulting equation is intractable. Hence, we adopt a lookup table approach as a practical alternative. To do this we tabulate $\cos(\theta_i)$ as a function of the computed diffuse intensity I from Eq. (5). Since the Lambertian reflectance I_L is proportional to $\cos(\theta_i)$, this allows us to approximate I_L using the measured intensity I. In practice, the larger the number of incidence angles tabulated ($0 \leq \theta_i \leq \frac{\pi}{2}$), the more precise the correction process. Once an approximate value of the surface slope

is estimated ($m = m_0$) using the technique outlined in Section 3, the lookup table is computed using Eq. (5).

Under conditions in which the viewer and light-source directions are almost identical, the modified B-K model is amenable to our lookup table approach since, like Lambert's law, the brightness decreases monotonically with increasing incidence angle (Fig. 1.a). As a result the reflectance function appearing in Eq. (5) are injective and invertible. In other words, each measured brightness value $I = I_0$ is related to a single value of incidence angle $\theta_i = \theta_0$ and hence to a single Lambertian reflectance value $I_L = \cos(\theta_0)$. Note also, that for other illumination geometries where the reflectance is dependent on both the incidence and reflectance angles, the lookup table approach is not usable.

5 Experiments

The images used in our experiments have been captured using an Olympus 10E camera. Each surface has been imaged under controlled lighting conditions in a darkroom. The objects have been illuminated using a single collimated tungsten light-source whose wavelength is approximately 700*nm*. The light-source direction is recorded at the time the images are captured. The objects used in our experiments are a terra-cotta bear and a cylindrical sandpaper.

5.1 Estimating Surface Slope

Our first experiment is to estimate surface slope *m* for rough surfaces (Section 3) composed of terra-cotta and sandpaper. First we need to measure two mean-intensity values I_1 and I_2 for two different angles of incidence θ_1 and θ_2. One way to do this is to use a small approximately planar patch on each object surface. However, if such planar patches can not be found, one may use a planar surface of the same material and roughness. For $\theta_1 = 30^\circ$, $\theta_2 = 45^\circ$ and $\lambda = 700nm$, we measure the mean-intensity ratio for the sandpaper $I_1/I_2 = 1.1004$ and for the terra-cotta $I_1/I_2 = 1.1147$. Hence, using Eq. (4) the surface slope is estimated $m = 1.41$ for the sandpaper and $m = 1.29$ for the terra-cotta.

5.2 Photometric Correction

The estimate of surface slope *m* allows us to fit the modified B-K model to the reflectance data for each object. The next experiment is to use the raw images of the terra-cotta bear and the cylindrical sandpaper together with the fitted models and perform photometric correction. Both raw images are captured under almost identical light-source and viewing directions. For each surface, we construct a lookup table, as described in Section 4, using the model of Eq. (5) and the value of surface slope *m* estimated for each surface. We present the results in Fig. 2. Here, the panels in the left-hand column show diffuse raw images (I), the panels in the second column show the recovered Lambertian images (I_L) and the panels in the third column show the difference images ($|I - I_L|$). Here, the darker the point in a difference image, the larger the difference. We use the absolute function to show both positive and negative differences. It can be seen in Fig. 1.a that for $m = 1.3$ (terra-cotta bear) if $\theta_i < 45^\circ$ then $I_L < I$, whereas for $m = 1.4$ (sandpaper), if $\theta_i < 60^\circ$ then $I_L < I$. Although the correction process has an effect at almost every location on each surface, the differences are most marked where the inclination of the object surface is steepest. To show the effects of the photometric correction process, we plot Lambertian intensity I_L versus original (raw) intensity I in the panels in the fourth column, and, $(I_L - I)$ versus I in the panels in the fifth column of Fig. 2. From these plots it is clear that for the sandpaper cylinder where $m = 1.41$ the decrease in intensity is much larger in magnitude

than for the terra-cotta bear where $m = 1.29$, while the increase is relatively stronger for the terra-cotta bear. For both objects, the difference in intensities is maximum for small intensities and is minimum for intermediate intensities.

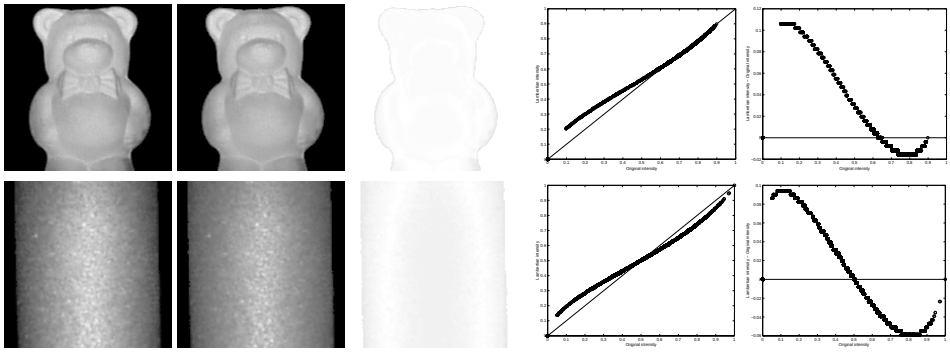

Figure 2: Photometric correction using the modified B-K model: original images (I), corrected Lambertian images (I_L), difference images ($I_L - I$), I_L versus I and $(I_L - I)$ versus I (left to right).

5.3 Shape-from-Shading and Re-illumination

Each corrected Lambertian image obtained in the last experiment can be used as an input image to shape-from-shading. Here we use the method of Worthington and Hancock [13]. This is a geometric technique which constrains the surface normals to fall on a cone whose axis points in the light-source direction and whose apex angle is the inverse cosine of the corrected Lambertian reflectance. The main reason for adopting this method is that it is relatively simple and makes the recovery of surface normal direction relatively straightforward. The needle maps of the surface normals obtained using this method are shown in Fig. 3. Here the panels in the left-hand column show the surface normals extracted from raw images whereas the panels in the centre column show those extracted from Lambertian images. The field of difference between these surface normals is shown in the panels in the right-hand column. Here, the complex surface structure of the terra-cotta bear, is clearly visible. For the sandpaper, the symmetrical shape of the cylinder is nicely preserved.

We now turn our attention in more detail to the effects of the Lambertian correction process on the surface normal directions. The changes in surface normal directions occur both in the zenith angles and in the azimuth angles. In qualitative terms, when the image becomes brighter then the apex (opening) angle of the Lambertian cone becomes smaller. Hence the zenith angle of the surface normal decreases. When the image becomes darker, on the other hand, then the zenith angle increases. To illustrate the effect of Lambertian correction process, we have produced scatter plots for the azimuth and zenith angles for surface normals extracted from the diffuse images I and the corresponding corrected Lambertian images I_L. In Fig. 4, the top row is for the terra-cotta bear whereas the bottom row is for the sandpaper cylinder. Here, the panels in the left-hand column show the scatter plots for the zenith angle, i.e. $\cos^{-1}(I_L)$ versus $\cos^{-1}(I)$, while the panels in the centre column show the scatter plots of the azimuth angle. In both scatter plots, the horizontal axis shows the angle extracted from the surface normals using I while the vertical axis shows the angle extracted from those using I_L. In the zenith angle plots, there is no scatter and the data points trace out a curve. The reason for this is that the Lambertian shape-from-shading method constrains the surface normals to fall on a cone whose apex

angle is the arc-cosine of the brightness. The axis of the cone points in the light-source direction, and since the light-source and viewing directions are identical, the apex angle of the cone is equal to the zenith angle. The azimuth angle plots, on the other hand, do exhibit scatter. The reason for this is that the surface normals are free to rotate about the cones subject to smoothness constraints. However, in each of the azimuth plots there is a clear regression line.

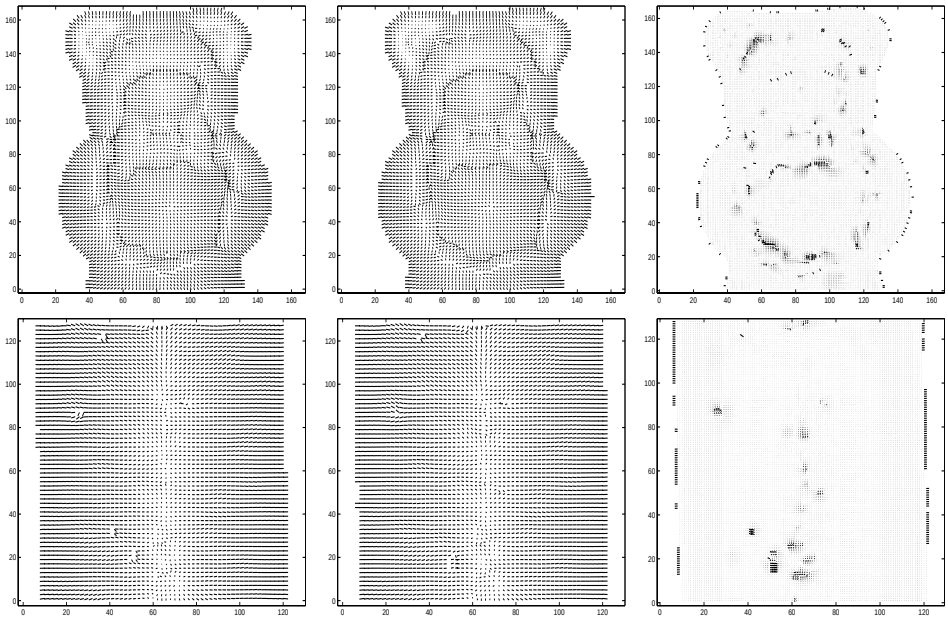

Figure 3: Needle maps of the surface normals obtained by applying shape-from-shading [13] to the raw images (left) and to the corrected Lambertian images (centre) which are shown in Fig. 2; The field of difference between the two needle maps (right).

To investigate the stability of the surface normals under changes in azimuth angle, the panels in the right-hand column show the difference in azimuth angle for the surface normals using I and I_L as function of the Lambertian zenith angle $\cos^{-1}(I_L)$. It is clear that the largest difference in azimuth angle occur at intermediate zenith angles. Hence, these are associated with reasonable changes in surface normal direction. This means that the modified B-K model results in significant differences in surface normal directions. Although this effect is mainly attributable to the larger differences in I_L, it may also reflect problems associated with the curvature dependant smoothing employed in the shape-from-shading algorithm. This uses the principal curvature direction to adjust the azimuth angle of the surface normal. When the surface is umbilic (e.g. at spheres) or hyperbolic (e.g. at saddles) there are singularities in the field of principal curvature directions and these in turn may lead to unstable azimuth angle estimates. It is also interesting to note that shape-from-shading results in small differences in azimuth angle for large zenith angles and near object limbs. The reason for this is that the boundary condition constrains surface normal to be perpendicular to the occluding boundary. This stability effect in the azimuth angles is distributed to the neighboring locations on the object limbs.

Once the accurate surface normals are in hand, re-illuminating object surfaces is a straightforward task. Since at each point on the surface, the local surface normal and

the viewing direction are known (and fixed), we can use the modified B-K model (Eq. 2) to compute the diffuse reflectance for any light-source direction. Using the surface normals extracted from the recovered Lambertian images (Fig. 3, centre), we experiment with re-illuminating surface objects from five different directions. In Fig. 5, we show re-illuminations of the two surface objects under study when the light-source direction is re-positioned. Here we move the direction of lighting on the image plane normal, in the horizontal direction. For the terra-cotta bear, again, we set $m = 1.29$ whereas for the cylindrical sandpaper we set $m = 1.41$. From the left-hand column to the right-hand column, the light-source directions are $(18^\circ, -90^\circ)$, $(9^\circ, -90^\circ)$, $(0, 0)$, $(9^\circ, 90^\circ)$ and $(18^\circ, 90^\circ)$ respectively, where the first and second numbers are the values of the zenith and azimuth angles. The images reflect the underlying shape of the object in a consistent manner.

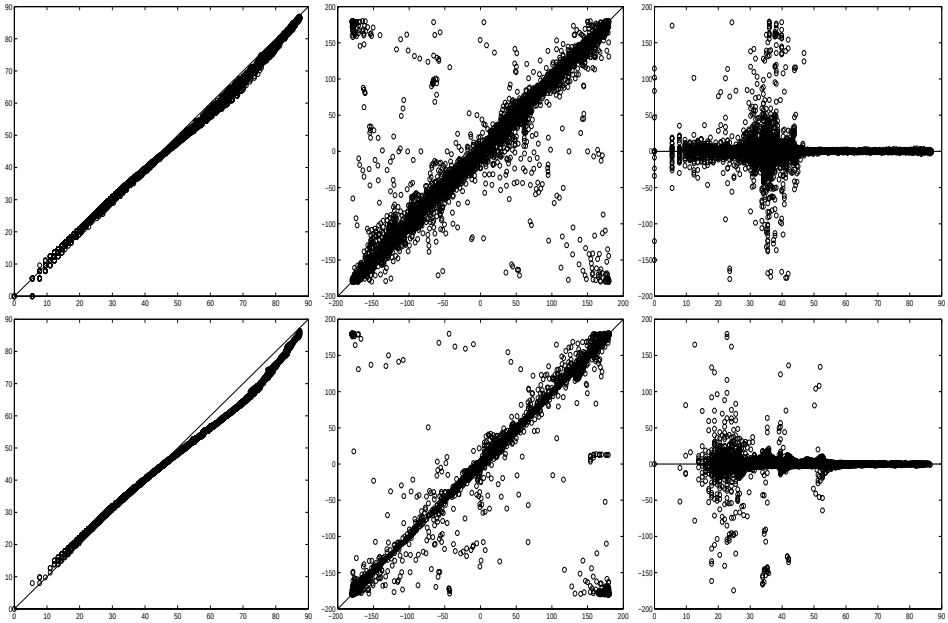

Figure 4: Plots for the incidence zenith (left) and azimuth (centre) angles (degrees) extracted from the recovered surface normals for the terra-cotta bear (top) and the sandpaper cylinder (bottom): the horizontal axis shows the angles extracted from the surface normals obtained by applying SFS to the diffuse image (Fig. 3, left), while the vertical axis shows those obtained by applying the same SFS method (and settings) to the Lambertian image (Fig. 3, centre); Plots for the difference between diffuse and Lambertian azimuth angles versus the Lambertian zenith angle (left).

6 Conclusions

In this paper, we have shown how the modified Beckmann-Kirchhoff model for very-rough surfaces can be used for surface slope estimation, photometric correction and re-illumination. The surface slope is estimated using a pair of images acquired under different illumination directions. Lambertian images are recovered from raw images by means of lookup tables computed using the fitted model for the objects illuminated nearly in the viewing direction. Once the Lambertian image is recovered, then the surface normals may be recovered using a Lambertian shape-from-shading method. Here, we show that photometric correction improves the accuracy of surface normals, and that by re-illuminating

these surface normals we generate realistic images. The results for this task are also interesting. Hence, the modified Beckmann-Kirchhoff model appears to offer an interesting alternative to existing rough reflectance models such as the Oren-Nayar model, and clearly has potential for applications beyond the scope of this paper.

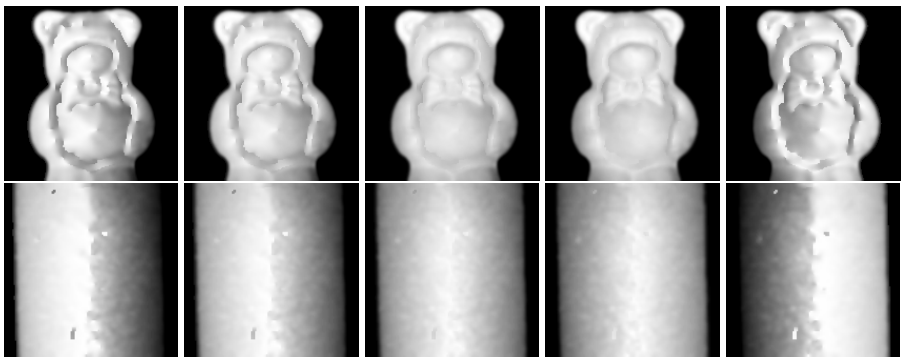

Figure 5: Diffuse images generated using the modified B-K model (Eq. 2) on the recovered surface normals (Fig. 3, centre) re-illuminated from five light-source directions: $(18^\circ, -90^\circ)$, $(9^\circ, -90^\circ)$, $(0, 0)$, $(9^\circ, 90^\circ)$ and $(18^\circ, 90^\circ)$, from left to right.

References

[1] D.E. Barrick. Rough surfaces scattering based on the specular point theory. *IEEE Trans. on Antennas Propagation*, 16:449–454, 1968.

[2] P. Beckmann and A. Spizzochino. *The scattering of electromagnetic waves from rough surfaces*. Pergamon Press Ltd., New York, 1963.

[3] J.M. Bennett and L. Mattsson. *Introduction to surface roughness and scattering*. Second Edition. Optical Society of America, Washington, D.C., 1999.

[4] J. Caron, J. Lafait, and C. Andraud. Scalar kirchhoff's model for light scattering from dielectric random rough surf. *Optics Communications*, 207:17–28, 2002.

[5] V.B. Ginneken, M. Stavridi, and J.J. Koenderink. Diffuse and specular reflectance from rough surfaces. *Applied Optics*, 37(1):130–139, 1998.

[6] X.D. He, K.E. Torrance, F.X. Sillion, and D.P. Greenberg. A comprehensive physical model for light reflection. *ACM Computer Graphics*, 25(4):175–186, 1991.

[7] S.K. Nayar, K. Ikeuchi, and T. Kanade. Surface reflection: Physical and geometrical perspectives. *IEEE Trans. on Pattern Analysis and Machine Intelligence*, 13(7):611–634, 1991.

[8] J.A. Ogilvy. *Theory of wave scatter. from random rough surf.* Adam Hilger, Bristol, 1991.

[9] H. Ragheb and E.R. Hancock. Lambertian correction for rough and shiny surfaces. In *Proc. International Conference on Image Processing*, pages 553–556, 2002.

[10] K.E. Torrance and E.M. Sparrow. Theory for off-specular reflection from roughened surfaces. *Journal of Optical Society of America*, 57(9):1105–1114, 1967.

[11] C.L. Vernold and J.E. Harvey. A modified Beckmann-Kirchoff scattering theory for nonparaxial angles. *Scattering and Surface Roughness, Proc. of the SPIE*, 3426:51–56, 1998.

[12] L.B. Wolff, S.K. Nayar, and M. Oren. Improved diffuse reflection models for computer vision. *International Journal of Computer Vision*, 30(1):55–71, 1998.

[13] P.L. Worthington and E.R. Hancock. New constraints on data-closeness and needle-map consistency for sfs. *IEEE Trans. Patt. Anal. Mach. Intell.*, 21(11):1250–1267, 1999.